ELSEVIER

Surface Science xxx (2002) xxx–xxx

SURFACE SCIENCE

www.elsevier.com/locate/susc

# STM studies of near-surface precipitation of gold in ultra-thin iron films on Au(0 0 1)

N. Spiridis [a], Józef. Korecki [a,b,*]

[a] *Institute of Catalysis and Surface Chemistry, Polish Academy of Sciences, 30-239 Kraków, Poland*
[b] *Department of Solid State Physics, Faculty of Physics and Nuclear Techniques, University of Mining and Metallurgy (AGH), al. Mickiewicza 30, 30-059 Kraków, Poland*

**Abstract**

Annealed 10 ML Fe films on Au(0 0 1) were studied using STM. Annealing above 670 K causes violent changes of the surface due to Au segregation. At 800 K annealing, formation of nanometer sized plate-like precipitates of gold in the Fe layer is observed. At higher temperatures the precipitates migrate and agglomerate. © 2002 Published by Elsevier Science B.V.

*Keywords:* Scanning tunneling microscopy; Molecular beam epitaxy; Surface structure, morphology, roughness, and topography; Surface segregation; Diffusion and migration; Iron; Gold

## 1. Introduction

Recent interest in magnetic nanostructures motivates intensive effort in tailoring objects with desired magnetic properties [1]. Atomic scale engineering often makes use of a specific growth, which may lead to contrasting behavior like self-organized nanostructuring [2] or self-surfactant action promoting a flat 2D-growth [3]. One of the best known examples of the latter are Fe films grown on Au(0 0 1) showing a flat growth mode, despite of unfavorable relations of surface energies [4]. The 2D-growth is promoted by the surface segregation of Au found even on the surface of a Fe film that is several tens of monolayers (ML) thick [5]. The segregation process is enhanced at elevated temperatures, and the mechanism was used to improve the quality of epitaxial Fe films [6]. On the other hand, a complex process of atom positions exchange during the vertical mass transport, which accompanies the segregation, may lead to intermixing between Au and Fe. Such intermixing and even complete dissolution is reported for Co films on Au [7]. At interfaces, due to finite interface energy and because of the lattice mismatch, strains and dislocations, the mobility of atoms is enhanced thus facilitating diffusion and migration. All the mentioned effects may lead to a strong deviation from the behavior predicted by a bulk phase diagram, especially upon annealing. It is both of fundamental and technological importance to study these processes in nanoscale. In this paper we report STM observations of the annealing induced morphology changes in Fe films

* Corresponding author. Address: Department of Solid State Physics, Faculty of Physics and Nuclear Techniques, University of Mining and Metallurgy (AGH), al. Mickiewicza 30, 30-059 Kraków, Poland. Tel.: +48-12-617-2911; fax: +48-12-634-1247.
*E-mail address:* korecki@uci.agh.edu.pl (J. Korecki).

0039-6028/02/$ - see front matter © 2002 Published by Elsevier Science B.V.
PII: S0039-6028(02)01202-5

grown on Au(0 0 1). At high annealing temperatures we observe a formation of regularly shaped naonostructures interpreted as Au precipitates.

## 2. Experimental and preparation of Au substrate

The experiment was performed in the UHV MBE system [8] equipped with home-built micro-MBE evaporators and the Aris1100 (Burleigh) STM head. As substrates we used $5 \times 10 \times 1$ mm$^3$ MgO(0 0 1) slices, cleaved in air prior to the introduction into the UHV system through a fast entry lock-load facility. The substrates were clamped to a Mo block being a part of a sample holder. A tungsten filament heated the sample radiatively and the sample temperature was measured using a Pt–RhPt thermocouple pressed against the Mo block. Au and Fe were evaporated from BeO crucibles heated by wrapped around tungsten coils. The evaporators were embedded in a water-cooled shroud. The deposition rate was calibrated referring to the indication of a quartz thickness monitor, which could be placed at a sample position. During the whole deposition process the pressure in the chamber was maintained in a low $10^{-8}$ Pa range.

Au(0 0 1) buffer layers were obtained forcing the Au epitaxy by a thin Fe seed layer. The topography and the surface structure of the Au films (30 nm was a standard thickness that ensured the electrical continuity) depended crucially on the deposition temperature and a post-preparation thermal treatment. Examples of STM images for the obtained structures are shown in Fig. 1. A non-reconstructed $1 \times 1$ (0 0 1) surface is typical of a high temperature (800 K) growth or annealing (Fig. 1a). Deposition at 450 K results in the Au(0 0 1)-*hex* surface typical of bulk Au [9]. The reconstructed surface of the best quality was obtained if a 3 nm Au layer was added at 450 K onto a film annealed at 800 K. The dominating defects seen on the reconstructed surface are straight or L-shaped steps, each of them terminated with a pair of screw dislocations. The density of the dislocations is about $2 \times 10^{10}$/cm$^2$ resulting in flat regular terraces, which are on the average 150 nm long and 20 nm wide. Other defects are small (about

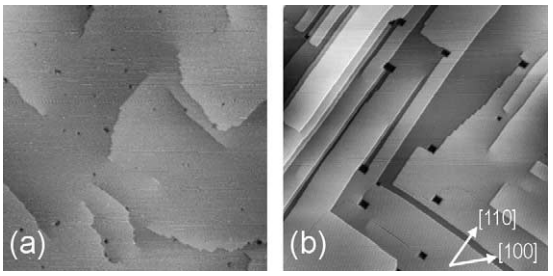


Fig. 1. $200 \times 200$ nm$^2$ STM topographs of the Au(0 0 1) buffer layer: (a) a $1 \times 1$ Au(0 0 1) surface annealed at 820 K and (b) reconstructed Au(0 0 1)-*hex* surface obtained after Au deposition at 420 K.

$6 \times 6$ nm$^2$) square holes, with quantized sizes and edge dislocations disturbing the reconstruction ridges. The terraces and the reconstruction ridges run always along ⟨1 1 0⟩ Au directions. The reconstruction, which is the same as for the Au(0 0 1) bulk surface, is roughly $5 \times 1$ (the ridges are spaced by 1.44 nm). The reconstruction means that a quasi-hexagonal Au surface layer is formed with the density higher by 20% than a $1 \times 1$ layer. Four types of domains with the reconstruction ridges in perpendicular directions are observed. The domains have different terminations: sometimes they meet and form a domain boundary at the same atomic level, and sometimes monoatomic steps separate them.

Increasing deposition or annealing temperature causes a transition from the reconstructed surfaces with a high density of steps and rectangular terraces to flatter and non-reconstructed ones with irregular terraces.

## 3. Fe films on Au(0 0 1)-*hex*

10 ML Fe films were evaporated at 300 K and annealed for 1 h at temperatures between 520 and 960 K. Auger spectra in Fig. 2 show the evolution of the Fe (47 eV) and Au (43/56/69 eV) lines with increasing annealing temperature. Already for the as-prepared sample the Auger spectrum indicates the presence of Au on top of the Fe layer. It is seen from the intensity ratio of the Au to Fe lines, which is about 1:10, compared to the expected 1:25 taking into account the Auger intensities from a

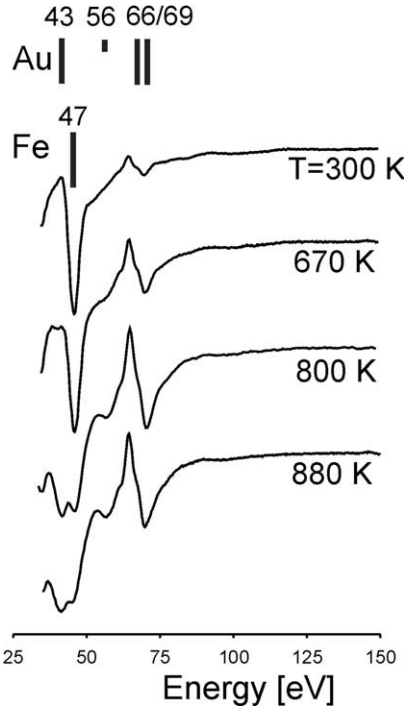


Fig. 2. Auger spectra for 10 ML Fe films on Au(0 0 1) as a function of annealing temperature.

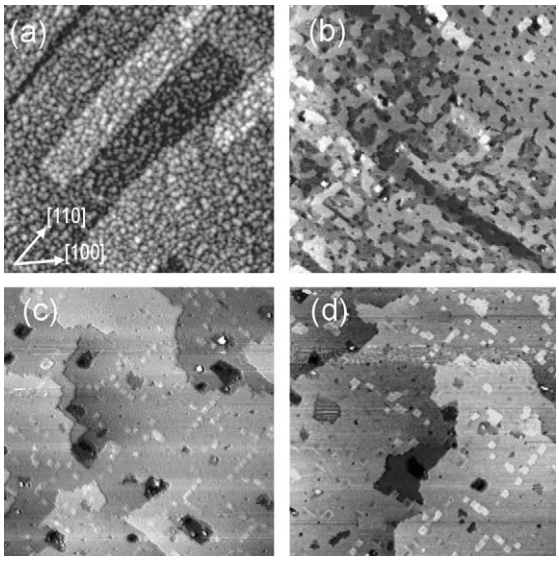


Fig. 3. $200 \times 200$ nm$^2$ STM topographs (typical tunneling conditions: sample bias $V_s = -50$ mV, tunneling current $I_T = 1$ nA) of a 10 ML Fe film on Au(0 0 1): (a) as-deposited and after 1 h annealing at (b) 670 K, (c) 800 K, (d) 880 K. Arrows indicate direction on the surface of the Au(0 0 1) buffer layer. Note that the Fe lattice is rotated by 45° relative to Au(0 0 1).

very thick sample and the inelastic mean free path of electrons with the appropriate energies [5]. The amount of Au increases rapidly at annealing temperatures higher than 520 K and nearly saturates at about 850 K. Annealing also causes considerable changes in LEED patterns, which reveal the re-appearance of the $5 \times 1$ Au(0 0 1) reconstruction for the samples annealed above 850 K. When Au is deposited on Fe(0 0 1) the $5 \times 1$ reconstruction emerges after completion of about 2 ML [10], which means that similar amount of Au must be present on the annealed 10 ML Fe films.

The most spectacular effect of annealing is observed in STM images as seen from Fig. 3, which shows topographic $200 \times 200$ nm$^2$ scans. For the as-deposited 10 ML film (Fig. 3a) the growth is rather flat, and the image is dominated by small (about 5 nm) monoatomic areas with three different atomic levels superimposed on a structure of the Au buffer steps. This observation agrees well with the previous STM [4] and spot profile LEED analysis [11]. Annealing at 670 K leads to surface flattening (Fig. 3b), as reported earlier [4]. Terraces become by one order of magnitude bigger and from the Auger analysis it is clear that the surface Au concentration increased considerably. More details are seen on smaller ($14 \times 14$ nm$^2$) scans in Fig. 4a. The surface seems to be chemically inhomogeneous and different step heights of about 0.05, 0.15 and 0.2 nm were found. The inhomogeneity is reflected also in a current image (Fig. 4c) that reveals atomic resolution, which can be obtained at low tunneling bias (below 25 mV) on irregular shallow concavities. We suggest that they correspond to the Au areas.

A further increase of annealing temperature up to 800 K causes violent changes of the surface morphology (Fig. 3c). The flat terraces become comparable to those observed for the surface of the Au(0 0 1) buffer layer annealed at high temperature (compare Fig. 1a). Various nano- and subnanoscale defects, whose appearance is very sensitive to the tunneling condition, are observed [12]. The most striking features are rectangular nanostructures in the form of islands or hollows.

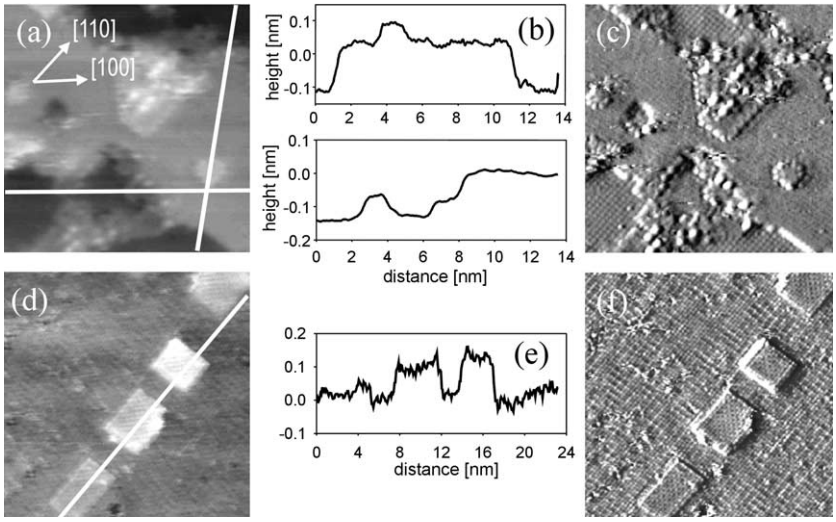


Fig. 4. Details of the surface structure for a 10 ML Fe film on Au(0 0 1) annealed for 1 h at 670 K (a)–(c) and 800 K (d)–(f). (a) $14 \times 14$ nm$^2$ topographic scan ($V_s = -20$ mV, $I_T = 1.3$ nA), (b) sections along the marked lines, (c) differentiated image shown in (a) to enhance the atomic resolution, (d) $20 \times 20$ nm$^2$ topographic scan ($V_s = -3$ mV, $I_T = 0.4$ nA), (e) section along the marked line, (f) differentiated image shown in (d).

The structures have the edges running along $\langle 1\,1\,0 \rangle$ directions of the Au lattice ($\langle 1\,0\,0 \rangle$ of Fe) and they tend to approach each other forming chains along the same direction. Details of the surface morphology are shown in Fig. 4d–f. The nanostructures have lateral dimensions 3–4 nm and a different height (depth) less than 0.12 nm. The atomic resolution, which can be obtained for the terraces as well as for the islands and hollows at the same tunneling condition reveals contrast fluctuations also observed for the $1 \times 1$ Au(0 0 1) surface and interpreted as the remainder of the *hex*-type reconstruction [8]. Rising annealing temperature up to 880 K causes an increase of the structure average dimension by 30% and enhances the tendency of agglomeration. Many of the nanostructures sinter but their original edges are still visible. Sometimes they stick to the step edges.

From the conversion electron Mössbauer measurements, which complemented the STM studies, we have found that the structural, electronic and magnetic properties of the Fe films do not change substantially during the annealing process [12]. The changes in the surface morphology did not affect seriously the Fe film, which remained continuous.

The nanostructures have a straightforward interpretation as Au plate-like precipitates in the Fe film. Their formation is the obvious consequence of the Au surface segregation. The vertical mass transport accompanying the segregation increases the amount of Au incorporated in the Fe film much above the bulk solubility limit. Annealing enhances the diffusion and facilitates reaching the equilibrium composition by precipitation of gold. It has to be remembered that, at annealing temperatures used, the surface of the Au buffer layer is also subjected to severe morphological modifications, which can contribute to the observed processes. The STM images reveal migration of the whole precipitates as well as their growth by atomic diffusion of Au. Our observations are in agreement with bulk diffusion of Au implanted in Fe single crystals, for which the formation of Au clusters was observed in a similar range of annealing temperatures [13].

The observed features of the Fe film surface can be easily explained by a simple model assuming the existence of plate-like subsurface Au precipitates with different numbers of atomic layers, laterally coherent with the Fe films, as shown in Fig. 5. A different height of the islands/hollows may be ob-

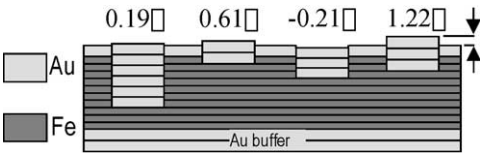


Fig. 5. Model of plate-like precipitates of Au in Fe films. Examples of Au precipitate causing protrusions (depression) on the surface depending on their height. Each rectangle represents a monoatomic layer, the aspect ratio of the precipitates is not to scale.

tained by stacking different number of Au layers with 10 atomic layers of the Fe film. The surface is covered additionally by at least one homogenous Au monolayer. Similar subsurface islands and fractional height differences, that do not correspond to the expected monoatomic steps, were observed previously for the growth of Cu on Pb(1 1 1), where 3D Cu islands were immersed in the Pb substrate and covered by a single Pb layer [14]. Here we have just the opposite situation, when the 3D precipitates of Au are formed from the substrate material in the deposited Fe film.

## 4. Conclusion

We have observed nano-sized precipitates of Au in a Fe film using STM. The STM images give an unambiguous evidence of the phase separation mechanism involving migration of the precipitates and their coalescence as suggested theoretically [15]. To our knowledge, for the first time the formation, coarsening and coalescence of precipitates in an alloy system have been visualized using STM, opening wide possibilities of further atomic scale studies of the phase separation kinetics.

## Acknowledgement

This work was supported by the State Committee for Scientific Research, grant no. 2 P03B 142 17.

## References

[1] F.J. Himpsel, J.E. Ortega, G.J. Mankey, R.F. Willis, Adv. Phys. 47 (1998) 511.
[2] B. Voigtländer, G. Meyer, N.M. Amer, Phys. Rev. B 44 (1991) 10354.
[3] F.J. Himpsel, Phys. Rev. B 44 (1991) 5966.
[4] V. Blum, Ch. Rath, S. Müller, L. Hammer, K. Heinz, Phys. Rev. B 59 (1999) 15966.
[5] A.M. Begley, S.K. Kim, J. Quinn, F. Jona, H. Over, P.M. Marcus, Phys. Rev. B 48 (1993) 1779.
[6] S. Bader, E.R. Moog, J. Appl. Phys. 61 (1987) 3729.
[7] S. Padovani, F. Scheurer, J.P. Bucher, Europhys. Lett. 45 (1999) 327.
[8] N. Spiridis, J. Korecki, Appl. Surf. Sci. 141 (1999) 313.
[9] X.-Q. Wang, Phys. Rev. Lett. 67 (1991) 3547.
[10] T. Ślęzak, private communication.
[11] Q. Jiang, Y.-L. He, G.-C. Wang, Surf. Sci. 295 (1993) 197.
[12] N. Spiridis, J. Korecki, to be published.
[13] A. Turos, O. Meyer, Phys. Rev. B 31 (1985) 5694.
[14] C. Nagl, E. Platzgummer, M. Schmid, P. Varga, S. Speller, W. Heiland, Phys. Rev. Lett. 75 (1995) 2976.
[15] K. Binder, D. Stauffer, Phys. Rev. Lett. 33 (1974) 1006.